

Visualising gravitational-wave event candidates using the Coherent Event Display[‡]

R. A. Mercer[§] and S. Klimenko

University of Florida, P.O. Box 118440, Gainesville, FL 32611, USA

E-mail: ram@gravity.phys.uwm.edu

Abstract. As a worldwide network of gravitational-wave detectors is now operating with an unprecedented sensitivity it is becoming increasingly important to be able to easily visualise gravitational-wave event candidates from various search pipelines using these detector networks. The Coherent Event Display (CED) has been developed with the goal of providing a simple and easy to use tool for performing follow up analyses of burst gravitational-wave event candidates. The CED produces a web page detailing reconstructed parameters, time-frequency maps, reconstructed detector responses, likelihood time-frequency maps, and reconstructed parameter skymaps. The CED supports events from all 2, 3, 4, and 5 detector network combinations of LIGO, GEO600, and Virgo.

Submitted to: *Class. Quantum Grav.*

1. Introduction

Over the past several years large scale laser interferometers have been used to search for gravitational-waves (GW) at a sensitivity level where signals from distant astrophysical sources may be seen. The three detector LIGO [1] network has attained its design sensitivity and the Virgo [2] and GEO600 [3] detectors are in the process of commissioning and are expected to achieve comparable sensitivities; as such it is becoming increasingly important to be able to easily visualise, and study events from various search pipelines running on data from these detector networks.

One type of search that is being actively pursued is for unmodelled signals [4, 5, 6, 7] that cannot be reliably searched for using matched filtering techniques, such as binary mergers and supernovae. The Coherent Event Display (CED) uses the search algorithms [8, 9] from the Coherent WaveBurst (cWB) pipeline [10], which has been designed to look for these unmodelled, or “burst”, GWs. The CED can therefore be used to investigate both burst GW event candidates, and accidental background events due to instrumental and environmental noise correlations by presenting reconstructed

[‡] Last Modified: 6 April 2008, Revision: 359

[§] Present address: University of Wisconsin-Milwaukee, P.O. Box 413, Milwaukee, WI 53201, USA

parameters, time-frequency maps, reconstructed detector responses, and reconstructed parameter skymaps in a simple yet easy to use package.

Section 2 describes the different components that make up the CED, Section 3 discusses the implementation and structure of the CED, and finally in Section 4 we summarise the main aspects of the CED.

2. Coherent Event Display Output Description

The Coherent Event Display (CED) is split up into several sections detailing different aspects of the requested event. This Section describes the contents of each of these sections, more detail can be found in the CED technical documentation [11].

2.1. Job and Event Parameters

The first two sections of the CED detail parameters specific to the analysis segment and the event in question. The GPS and UTC start times of the analysis segment used is reported along with parameters reconstructed using the cWB pipeline, a description of some of these parameters can be found below. A complete description of all the reconstructed parameters can be found in the CED Technical Documentation [11].

- The first series of parameters that are displayed are related to the time at which the event occurs. The start, stop, and central GPS times are recorded along with the central time relative to the start of the data segment used.
- Another parameter that is displayed in the event parameters table is h_{rss} which represents the reconstructed GW strain from the event in question.
- The likelihood is the main coherent statistic that the cWB algorithms, and therefore the CED, uses to identify events. The likelihood is defined as the total detected energy and is given in Equation 1:

$$\mathcal{L} = \sum_{ij} \sum_{k=1}^K \frac{1}{\sigma_k^2 [i, j]} \left[w_k^2 [i, j] - (w_k [i, j] - \xi_k [i, j])^2 \right] \quad (1)$$

$\sigma_k^2 [i, j]$ is the variance of the data from the k th detector, at time index i and frequency index j ; $w_k [i, j]$ is the sampled detector data; and $\xi_k [i, j]$ is the detector response.

- Another reported parameter is the network correlation, in order to understand what this parameter represents we first need to consider the total detected energy, Equation 1, which can be rewritten as:

$$\mathcal{L} = \sum_{m,n} C_{mn} \langle w_m w_n \rangle \quad (2)$$

where m and n index the multiple detectors that make up the network, C_{mn} are the correlation coefficients, and $w_{m,n}$ is the detector output for the given detector.

This detected energy can be split up into two distinct types of energy, incoherent and coherent:

$$\sum_{m,n} C_{mn} \langle w_m w_n \rangle = E_{m=n} + E_{m \neq n} \quad (3)$$

where the diagonal terms, $m = n$, correspond to the incoherent energy, and off-diagonal terms, $m \neq n$, the coherent energy. The network correlation can then be defined as:

$$C_{\text{net}} = \frac{E_{m \neq n}}{E_{\text{Null}} + E_{m \neq n}} \quad (4)$$

where E_{Null} represents the total normalised energy of the reconstructed detector noise. The network correlation, C_{net} , is used for the post-production selection of triggers, as a GW event should have a high value of network correlation whereas a accidental coincidence will have a lower value.

- Another series of parameters that are displayed are ϕ and θ , these record the reconstructed sky location for the detected event, as weighted by the likelihood. The coordinate system is the Earth fixed frame with $\phi = 0^\circ$ corresponding to the Greenwich Meridian, $\theta = 90^\circ$ corresponding to the equator, and $\theta = 0^\circ$ corresponding to the south pole.

2.2. Time-Frequency Maps

The next section of the CED displays time-frequency maps, these show the wavelet coefficients normalised by the noise RMS as a function of time and frequency for the event in question.

2.3. Likelihood Time-Frequency Maps

The next section of the CED contains the likelihood time-frequency maps, these plots show the likelihood, defined in Equation 1, as a function of time and frequency for the entire detector network for the event in question. Figure 1 shows an example likelihood time-frequency map, created after running the CED on a 46-46 M_\odot phenomenological BBH injection.

The above likelihood time-frequency map has been generated using the default ‘‘Pixel’’ plotting style. Two other plotting styles are available: ‘‘Shaded’’ which interpolates between adjacent data points to give a smoother appearance to the map, and ‘‘Cluster’’ which reconstructs only the event cluster requested.

2.4. Reconstructed Detector Responses

The next section of the CED display plots showing the reconstructed detector responses. There are three types of plot, the first of which shows the reconstructed strain for the detected event. An example reconstructed strain plot can be seen below in Figure 2,

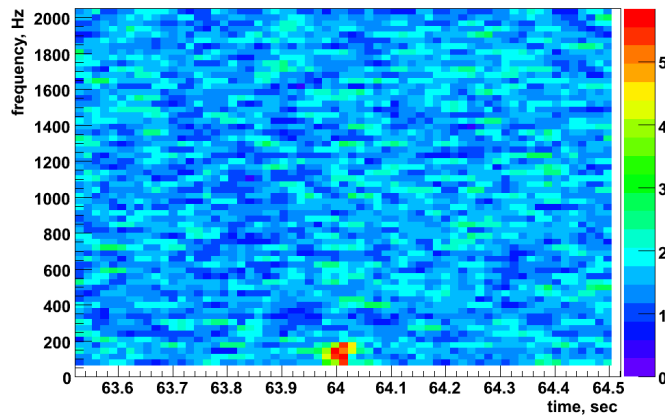


Figure 1. An example likelihood time-frequency map from the Coherent Event Display run on a 46-46 M_{\odot} phenomenological BBH injection.

this plot was created by running the CED on a 46-46 M_{\odot} phenomenological [12, 13] BBH injection.

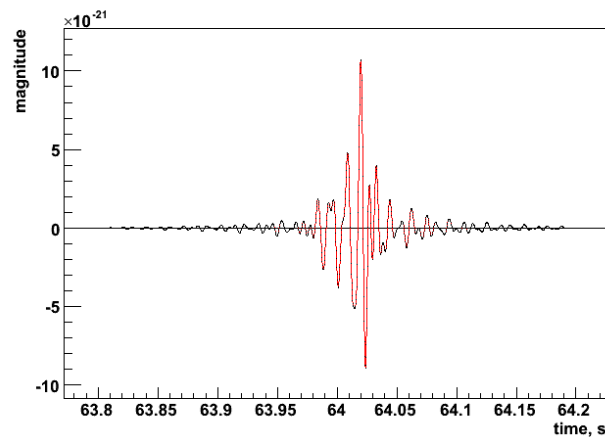


Figure 2. An example reconstructed strain signal plot from the Coherent Event Display run on a 46-46 M_{\odot} phenomenological BBH injection for the 4 km LIGO Livingston interferometer.

The other two plots that are displayed in the reconstructed detector response section contain two different reconstructed waveforms, the reconstructed strain and the band limited detector output. The first of these remaining plots shows the detector response and strain reconstructed using the reconstructed signal. The second, again, shows the detector response and the strain, this time reconstructed using both the signal and the noise.

2.5. Skymaps

Several of the parameters reconstructed by the CED have a dependency on the sky location, these parameters are presented as a function of the sky location as a series of skymaps showing the value of the reconstructed parameter at a given sky location. The first two of which shows the sensitivity of the detector network to the plus and cross polarisations as a function of sky location. In order to understand what these skymaps represent, it is necessary to introduce the antenna pattern vectors, given below in Equation 5:

$$\mathbf{f}_{+(\times)}[i, j] = \left\{ \frac{F_{1+(\times)}[i, j]}{\sigma_1[i, j]}, \dots, \frac{F_{K+(\times)}[i, j]}{\sigma_K[i, j]} \right\} \quad (5)$$

where $F_{k+(\times)}[i, j]$ are the antenna patterns, of the k th detector, for the $+$ and \times polarisations. These antenna pattern vectors $\mathbf{f}_{+(\times)}[i, j]$ are defined in the Dominant Polarisation Frame [8] and the norms of these vectors, $|\mathbf{f}_+|^2$ and $|\mathbf{f}_\times|^2$ represent the sensitivity of the detector network to the $+$ and \times polarisations respectively. An example cross polarisation skymap can be seen below in Figure 3, this was created by running the CED on a 46-46 M_\odot phenomenological BBH injection.

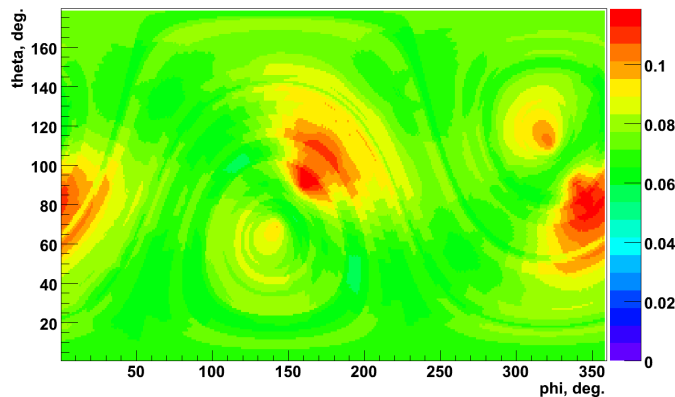


Figure 3. An example network sensitivity skymap, showing the sensitivity of the detector network to the cross polarisation, created after running the Coherent Event Display on a 46-46 M_\odot phenomenological BBH injection.

The next skymap shows the penalty factor as a function of sky location; in order to understand what this skymap represents it is necessary to introduce one of the constraints used in the analysis, the signal-noise orthogonality requirement, given below in Equation 6:

$$\Lambda_k = \sum_{ij} \left(w_k[i, j] s_k[i, j] - s_k^2[i, j] \right) = 0 \quad (6)$$

where $w_k[i, j]$ is the sampled detector data for the k th detector, at time index i , and frequency index j ; and $s_k[i, j]$ is the whitened detector response for the k th detector,

at time index i , and frequency index j . The reason for this constraint is to prevent the reconstruction of unphysical detector responses when the energy of the response is greater than the total energy in the detector data, i.e. $E_k > S_k$ where E_k is the total energy in the detector data; and S_k is the energy of the reconstructed detector response, given by Equation 7.

$$E_k = \sum_{ij} w_k^2 [i, j], \quad S_k = \sum_{ij} s_k^2 [i, j] \quad (7)$$

This constraint, Equation 6, is applied during the likelihood variation procedure of the cWB pipeline in the form of the penalty factor, by penalising sky locations where this constraint is not satisfied, i.e.:

$$P_k = \begin{cases} \sqrt{E_k/S_k} & : E_k < S_k \\ 1 & : E_k > S_k \end{cases} \quad (8)$$

where P_k is the penalty factor for the k th detector, therefore the overall penalty factor P_f is given by the maximum value of P_k :

$$P_f = \max_k P_k \quad (9)$$

it is this quantity P_f that is plotted as a function of sky location in order to generate the penalty factor skymap.

The next skymap shows the maximum value of the network correlation, Equation 4, as a function of sky location. An example network correlation skymap can be seen below in Figure 4, this skymap was created by running the CED on a 46-46 M_\odot phenomenological BBH injection.

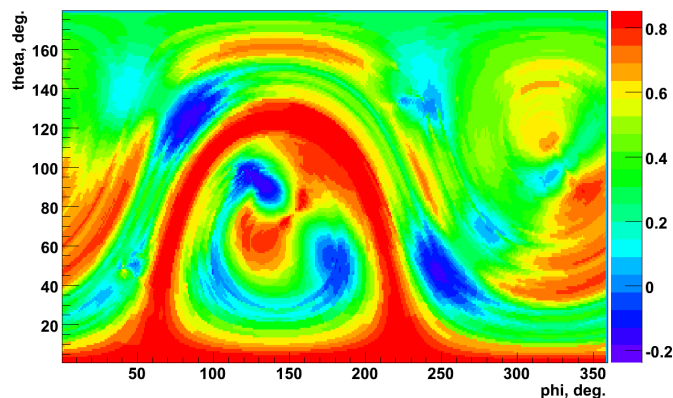


Figure 4. An example network correlation skymap created after running the Coherent Event Display on a 46-46 M_\odot phenomenological BBH injection.

The next skymap shows the maximum value of the likelihood, Equation 1, as a function of sky location. One problem with the likelihood skymap is that it does not take in account the detector response, therefore regions with high likelihood could correspond

to sky locations to which the detector network has a limited sensitivity. As it is unlikely that a real GW signal will be detected from these regions of limited sensitivity the likelihood does not provide an accurate statistic on which to claim detection. For this purpose the sky statistic is introduced, this can be considered to be the likelihood weighted with the detector response and is given by:

$$\text{Sky Stat} = \mathcal{L} P_f C_{\text{net}} \quad (10)$$

where \mathcal{L} is the likelihood, P_f the penalty factor (defined in Equation 9), and C_{net} the network correlation coefficient (defined in Equation 4). An example sky statistic skymap can be seen below in Figure 5, this skymap was created by running the CED on a 46-46 M_{\odot} phenomenological BBH injection.

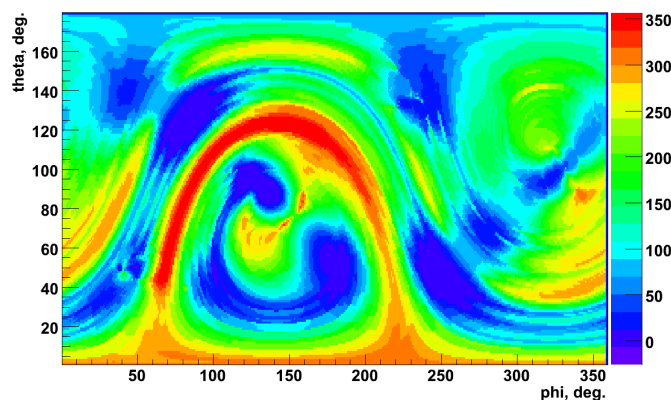


Figure 5. An example sky statistic skymap created after running the Coherent Event Display on a 46-46 M_{\odot} phenomenological BBH injection.

As shown in Equations 2 and 3 the total energy can be considered to be made of two components, $E_{m=n}$ the incoherent energy, and $E_{m \neq n}$ the coherent energy. The next skymap shows the coherent energy $E_{m \neq n}$, sometimes referred to as the correlated energy, as a function of sky location. An example correlated energy skymap can be seen below in Figure 6, this skymap was created by running the CED on a 46-46 M_{\odot} phenomenological BBH injection.

Another way that the likelihood, Equation 1, can be written is in term of the normalised and reconstructed energies: $\mathcal{L} = E - N$ where E the total normalised energy in the detector output, and N is the total reconstructed energy of the noise, given in Equation 11:

$$E = \sum_{ij} |\mathbf{w}[i, j]|^2, \quad N = \sum_{ij} |\mathbf{w}[i, j] - \mathbf{s}[i, j]|^2 \quad (11)$$

where the vector $\mathbf{w}[i, j]$ is defined by:

$$\mathbf{w}[i, j] = \left\{ \frac{w_1[i, j]}{\sigma_1[i, j]}, \dots, \frac{w_K[i, j]}{\sigma_K[i, j]} \right\} \quad (12)$$

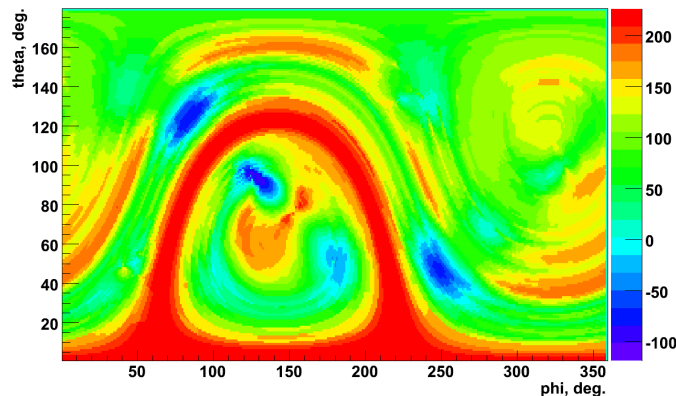


Figure 6. An example correlated energy skymap created after running the Coherent Event Display on a 46-46 M_{\odot} phenomenological BBH injection.

and the vector $\mathbf{s}[i, j]$ is defined by:

$$\mathbf{s}[i, j] = \left\{ \frac{\xi_1[i, j]}{\sigma_1[i, j]}, \dots, \frac{\xi_K[i, j]}{\sigma_K[i, j]} \right\} \quad (13)$$

The quantity N is called the null stream and is plotted, as a function of sky location, as the null energy skymap; an example of which can be seen below in Figure 7, this skymap was created by running the CED on a 46-46 M_{\odot} phenomenological BBH injection.

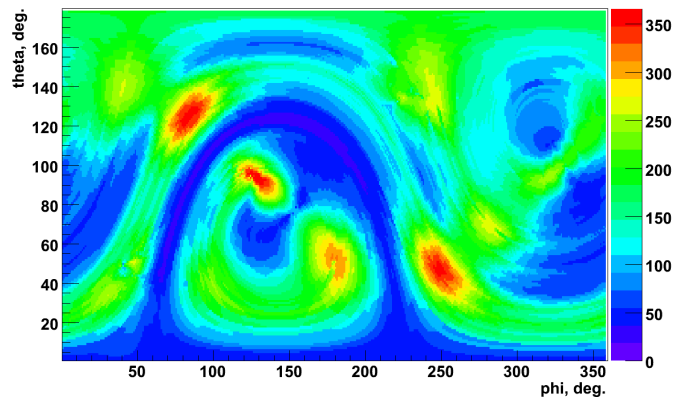


Figure 7. An example null energy skymap created after running the Coherent Event Display on a 46-46 M_{\odot} phenomenological BBH injection.

As discussed earlier, one of the constraints that is applied during the analysis is the signal-noise orthogonality requirement given by Equation 6. This constraint is applied to the likelihood by means of the penalty factor, Equation 9, not by rigidly enforcing the constraint. The energy disbalance skymap shows the sum, over detectors, of Λ_k as a function of sky location.

The final skymap shows the normalisation factor, this is an internal check to ensure that the likelihood calculation is being performed correctly. If any region of this is not equal to unity then that indicates that there is a problem with the chosen parameters.

3. Implementation

The Coherent Event Display (CED) is built on top of the Coherent WaveBurst (cWB) algorithms and as such shares a lot of the properties of the main cWB search pipeline. This section briefly discusses how the CED is implemented using aspects of the cWB pipeline, more detailed information can be found within the CED Technical Documentation [11].

3.1. Execution Environment

The CED is controlled through a single driver script which ensures that the system environment is correctly setup so that the ROOT framework [14], the LIGO/Virgo Frame Library [15], and the Wavelet Analysis Tool (WAT) [10] are available prior to starting the main analysis loop taken from the cWB pipeline.

Once it has been established that the execution environment is correctly setup the CED is started, details of the requested event are read in and an appropriate data stretch is determined and located.

3.2. Identifying the Event

As the main analysis loop of the CED is the same as used in the cWB pipeline there may be multiple events detected in the chosen analysis segment. Only one of these events will be the requested event, it therefore needs to be determined which of these multiple events is the appropriate one.

This is done by stepping through the list of detected events and checking if the central time of the event, in each detector of the network, is contained within the range of times specified. If multiple events are found that match the supplied parameters then the CED chooses the event which has the highest likelihood, as it is more probable that this event will be of more interest.

3.3. Parameter, Plot, and Website Production

Once the requested event has been successfully identified all the appropriate parameters are recorded and the CED can now generate various plots illustrating the event, such as time-frequency maps, reconstructed detector responses, and reconstructed parameter skymaps. Finally the end product of CED, a website, can be constructed.

4. Summary

In this paper we have discussed the structure, layout, and implementation of the CED and seen that it can be used for follow up analyses of both burst GW event candidates and accidental environmental or instrumental noise correlations. We have shown that the CED provides a simple, easy to use, tool that presents reconstructed parameters, time-frequency maps, reconstructed detector responses, and reconstructed parameter skymaps in a single package, the output of which can be easily viewed, and explored, using nothing more than a web browser.

References

- [1] D Sigg (for the LSC). Status of the LIGO detectors. *Classical and Quantum Gravity*, 23:S51, 2006.
- [2] F Acernese et al. Status of VIRGO. *Classical and Quantum Gravity*, 23:S63, 2006.
- [3] H Lück et al. Status of the GEO600 detector. *Classical and Quantum Gravity*, 23:S71, 2006.
- [4] B. Abbott et al. (LIGO Scientific Collaboration). First upper limits from LIGO on gravitational-wave bursts. *Physical Review D*, 69:102001, 2004.
- [5] B. Abbott et al. (LIGO Scientific Collaboration). Upper limits on gravitational-wave bursts in LIGO's second science run. *Physical Review D*, 72:062001, 2005. gr-qc/0505029.
- [6] B. Abbott et al. (LIGO Scientific Collaboration). Search for gravitational-wave bursts in LIGO's third science run. *Classical and Quantum Gravity*, 23:S29, 2006. gr-qc/0511146.
- [7] B. Abbott et al. (LIGO Scientific Collaboration). Search for gravitational-wave bursts in LIGO data from the fourth LSC science run, 2007. arXiv:0704.0943.
- [8] S. Klimenko et al. Constraint likelihood analysis for a network of gravitational wave detectors. *Physical Review D*, 72:122002, 2005.
- [9] S. Klimenko et al. Coherent method for detection of gravitational wave bursts, 2008. LIGO-T070093-00-Z.
- [10] S. Klimenko et al. Coherent WaveBurst - WAT version 4.7.0, 2008. LIGO-T080011-00-Z.
- [11] R. A. Mercer and S. Klimenko. The Coherent Event Display, 2008. LIGO-T080077-00-Z.
- [12] P. Ajith et al. A template bank for gravitational waveforms from coalescing binary black holes: I. non-spinning binaries, 2007. arXiv:0710.2335.
- [13] D. A. Brown et al. Data formats for numerical relativity waves, 2007. arXiv:0709.0093.
- [14] <http://root.cern.ch>.
- [15] <http://lappweb.in2p3.fr/virgo/FrameL>.